NANO LETTERS

pubs.acs.org/NanoLett Letter

Efficiency Roll-Off Free Electroluminescence from Monolayer WSe_2

Shiekh Zia Uddin,[†] Naoki Higashitarumizu,[†] Hyungjin Kim, I. K. M. Reaz Rahman, and Ali Javey*

Cite This: *Nano Lett.* 2022, 22, 5316–5321 Read Online

ACCESS | Metrics & More | Article Recommendations | Supporting Information

ABSTRACT: Exciton–exciton annihilation (EEA) is a nonradiative process commonly observed in excitonic materials at high exciton densities. Like Auger recombination, EEA degrades luminescence efficiency at high exciton densities and causes efficiency roll-off in light-emitting devices. Near-unity photoluminescence quantum yield has been demonstrated in transition metal dichalcogenides (TMDCs) at all exciton densities with optimal band structure modification mediated by strain. Although the recombination pathways in TMDCs are well understood, the practical application of light-emitting devices has been challenging. Here, we demonstrate a roll-off free electroluminescence (EL) device composed of TMDC monolayers tunable by strain. We show a 2 orders of magnitude EL enhancement from the WSe_2 monolayer by applying a small strain of 0.5%. We attain an internal quantum efficiency of 8% at all injection rates. Finally, we demonstrate transient EL turn-on voltages as small as the band gap. Our approach will contribute to practical applications of roll-off free optoelectronic devices based on excitonic materials.

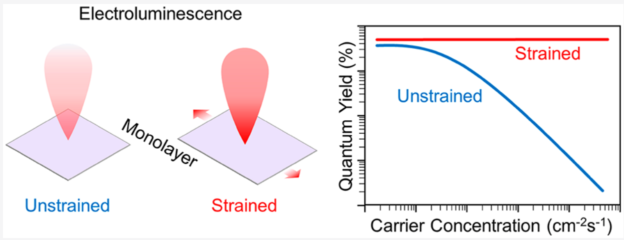

KEYWORDS: *electroluminescence, exciton–exciton annihilation, strain, efficiency roll-off*

Monolayer transition-metal dichalcogenides (TMDCs) have attracted tremendous attention toward optoelectronic applications at the ultimate scale thickness. Although as-exfoliated or as-grown monolayer TMDCs typically show a low photoluminescence (PL) quantum yield (QY) of 0.1–1%, their PL QY can approach near-unity at the low generation rates when nonradiative trion recombination is suppressed by electrostatic or chemical counterdoping.[1,2] At the high generation rates, however, PL QY in the TMDC monolayer significantly drops due to exciton–exciton annihilation (EEA). EEA is generally observed in all excitonic materials including organic and some inorganic semiconductors.[3,4] EEA is primarily responsible for the efficiency roll-off and limits the performance of light-emitting and light-harvesting device applications at high brightness. Recently, we reported that EEA is enhanced when van Hove singularity (VHS) resonance occurs at twice the exciton transition energy in the joint density of states (JDOS).[5] A relatively small strain of ~0.4% can move VHS resonance away from resonance and suppress EEA, leading to near-unity PL QY at all exciton densities. However, the roll-off free light-emitting devices based on TMDC monolayers have still been challenging.

Many electroluminescence (EL) devices based on TMDC monolayers have been reported in the literature, such as *p*–*n* junction,[6−14] quantum well (QW),[15−17] thermal emission,[18,19] and metal–insulator–semiconductor (MIS)[20,21] structures. The external quantum efficiency (QE) is lower than 1% in most cases,[6,7,9,13,22,23] and efficiency roll-off has been observed in WS_2 EL devices with the MIS structure.[21] Although a relatively high external QE of around 1–10% has been reported with the use of a complex quantum well structure of graphene/*h*-BN/TMDC/*h*-BN/graphene, bipolar ohmic contact is still challenging.[15,16] A transient-mode EL device, which consists of a simple capacitor structure with a single source contact, can achieve a large band bending enabling a high injection current rate during the gate voltage transient regardless of the Schottky barrier height.[24−28] Here, we demonstrate a roll-off free transient-mode EL device based on TMDC monolayers. The PL QY of WSe_2 monolayers reaches near-unity even at high exciton density by applying external tensile strain together with gate modulation due to the inhibition of VHS resonance. With the application of a small strain of 0.5%, notably, the WSe_2 monolayer shows an EL enhancement by 2 orders of magnitude, and its internal QE reaches 8% at maximum, without efficiency roll-off. We also demonstrate turn-on voltages in the order of the optical band gap in our transient EL devices. Our approach will contribute to practical applications of high-efficiency, high-brightness optoelectronic devices based on excitonic materials.

To control electrostatic counterdoping and mechanical strain, we utilized a conventional gate oxide on a thermally stable polymer substrate, which is more process-friendly and can be enlarged to a wafer-scale compared to a two-

Received: March 31, 2022
Revised: June 16, 2022
Published: June 22, 2022

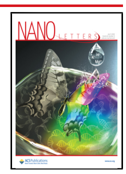

https://doi.org/10.1021/acs.nanolett.2c01311
Nano Lett. 2022, 22, 5316–5321

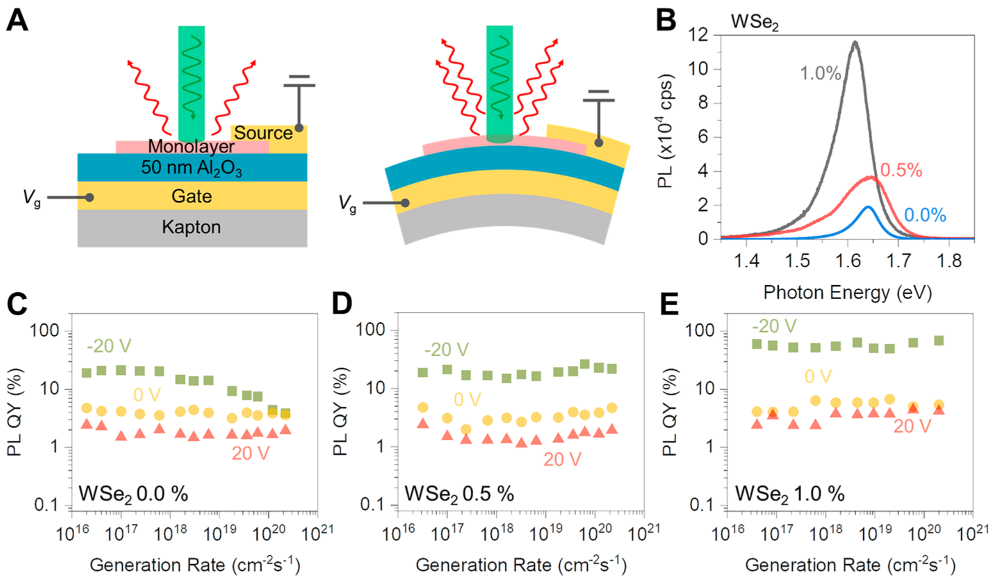

Figure 1. Near-unity PL QY in WSe_2 at all generation rates. (A) Schematic of the device used to explore PL from monolayers. (B) Typical PL spectra of monolayer WSe_2 under different uniaxial strains of ϵ = 0%, 0.5%, and 1.0%, at a high generation rate of $G = 2.2 \times 10^{20}$ cm^{-2} s^{-1} and gate voltage of $V_g = -20$ V. (C−E) PL QY in monolayer WSe_2 at different generation rates, gate voltages, and strains.

dimensional heterostructure with graphene and *h*-BN flakes fabricated on plastic substrates.[5] We first explore the PL QY of TMDC monolayers with an optimization of the background carrier concentration, generation rate, and band structure. Figure 1A shows a schematic of the strain tunable device used in PL measurements. Ti (10 nm)/Au (100 nm)/Ti (10 nm) was deposited on a 1.5 mm thick polyimide substrate (Kapton, Dupont) as a gate electrode, followed by an atomic layer deposition (ALD) of 50 nm Al_2O_3 at 200 °C as a gate insulator. 50 nm thick Au source electrodes were patterned on ALD oxide adjacent to gate electrodes. Monolayer WSe_2 was grown on a SiO_2/Si substrate via chemical vapor deposition (CVD)[25] and was then dry-transferred onto the ALD oxide using poly(methyl methacrylate) (PMMA) as a transfer medium. Exfoliated few-layer graphene (Graphenium, NGS Naturgraphit) was transferred by PMMA, bridging the monolayer and source electrode. A tensile strain was applied in the monolayer by a linear actuator. The nominal applied strain was calculated using the equation $\epsilon = t/R$, where $2t$ and R are the substrate thickness and curvature radius. Micro-PL measurements were performed at room temperature using a 514.5 nm excitation laser. Figure 1B shows PL spectra of monolayer WSe_2 under different applied strains at a high generation rate and negative gate voltage of $G = 2.2 \times 10^{20}$ cm^{-2} s^{-1} and $V_g = -20$ V, respectively. Generation rate G is the number of excitons created or the number of photons absorbed per unit area per unit time, which can be tuned by changing the laser intensity. The PL peak position red-shifted with an increase in the applied strain, confirming that the external strain is effectively transferred into the monolayer in this structure (a similar spectrum change obtained for WS_2 is shown in Figure S1).

The PL QY of TMDC monolayers generally decreases at high generation rates because of EEA.[1,5] Figure 1C−E shows the PL QY in monolayer WSe_2 at different generation rates and electrostatic counterdoping under different applied strains of ϵ = 0.0%, 0.5%, and 1.0%. As the exfoliated monolayer WSe_2 is naturally electron doped because of sulfur vacancies, thus a negative gate voltage is required to make it neutral.[2] Without applied strain, the PL QY increases by an order of magnitude at low generation rates when the negative gate voltage of $V_g = -20$ V is applied, suppressing nonradiative recombination of negatively charged trions by making the Fermi level neutral. At higher generation rates above $G = 10^{18}$ cm^{-2} s^{-1}, the PL QY drops due to the EEA.[5] With increasing applied strain, the PL QY for neutral excitons ($V_g = -20$ V) increases and approaches near-unity at all generation rates, as shown in Figure 1D,E. Similar with WSe_2, a roll-off free PL QY was achieved in monolayer WS_2 (Figure S2). These enhancements are comparable to the strained TMDC monolayers gate-modulated with *h*-BN and graphene heterostructures,[5] indicating a successful strain transfer and gate modulation into the emitting layers in the present device structure.

In order to evaluate the EL performance while systematically changing the strain, the transient mode EL[24,25] was measured using a bipolar sine wave applied to the gate electrode while the source electrode was grounded (Figure 2A). The flexible device used in the EL measurement was the same structure as that for the PL measurement. Monolayer WSe_2 EL devices were measured under nitrogen flow to prevent degradation. By applying moderate strain, VHS resonance is inhibited at twice the exciton transition energy E_X in the JDOS, suppressing EEA (Figure 2B,C).[5] Figure 2D shows typical EL spectra with the applied strain of ϵ = 0% and 0.5% under the fixed gate voltage and operating frequency at V_g = 22.5 V and 100 kHz, respectively. With no strain, the EL peak was observed at 1.66 eV, which is consistent with the PL peak position (Figure 1B). By applying 0.5% strain, the EL peak red-shifted to 1.61 eV, and its intensity was enhanced by over 2 orders of magnitude. For further investigation, the calibrated EL internal efficiency was measured[24] as a function of gate voltage, average carrier injection rate, and applied strain. Although an accurate measurement of carrier injection is difficult because of the small device size of around 50−100 μm, the external QE can be approximately estimated as a ratio of the number of output EL photons to number of injected carriers. In the present capacitor structure, the total injected carrier density when the gate voltage is swept from $-V_g$ to $+V_g$ is given by[24]

https://doi.org/10.1021/acs.nanolett.2c01311
Nano Lett. 2022, 22, 5316−5321

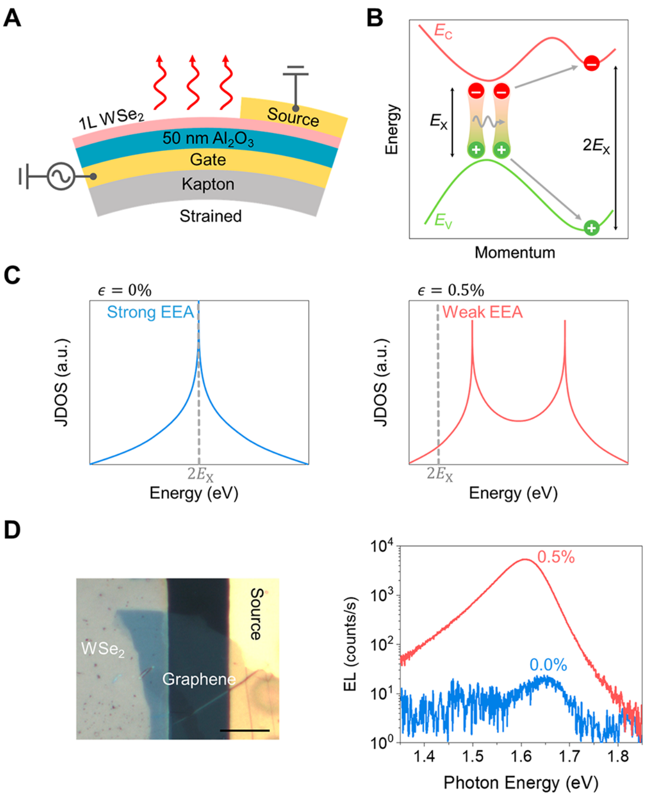

Figure 2. Tunable EL from monolayer WSe_2. (A) Schematics of a strain tunable transient mode EL device based on monolayer WSe_2. (B) Schematic diagram of the EEA process: nonradiatively transferring energy and momentum between two excitons. (C) Schematic diagram of the joint density of states at twice the exciton transition energy E_X, which determines the EEA rate. By applying moderate strain, $2E_X$ has no overlap with VHS resonance, resulting in EEA suppression. (D) Optical image of a strain tunable device and typical EL spectra from monolayer WSe_2 at different strains of ϵ = 0% and 0.5%. The scale bar is 5 μm. Gate voltage and operating frequency were fixed at V_g = 22.5 V and f = 100 kHz, respectively.

$$n_0 + p_0 = C_{ox}(2V_g - E_g/q)/q$$

where n_0 and p_0 are the steady-state electron and hole concentrations corresponding to a positive and negative V_g, respectively, C_{ox} is the areal gate capacitance, and q is the elementary charge. When an alternating current is applied at the frequency f, the carrier injection rate Q can be written as

$$Q = f(n_0 + p_0)$$

The external QE can be extracted by dividing the emitted EL photons per unit by carrier injection rate and can then be converted to internal QE by dividing by the light extraction efficiency of $1/4n^2$, where n is the refractive index of the Al_2O_3.[24,25] Figure 3A shows the EL internal QE of monolayer WSe_2 with no strain. EL efficiency monotonically increases from 5.0 to 10.0 V and is then saturated at over 12.5 V (Figure S3), which is consistent with the previous report on monolayer WS_2 and WSe_2 EL devices.[24] The maximum EL efficiency was around ~3% at the low carrier injection rate. At a higher carrier injection rate of over mid-10^{17} cm^{-2} s^{-1}, the EL QE dramatically decreases by 2 orders of magnitude, like the PL QY as a function of generation rate (Figure 1C). The typical EL internal QE was on the order of 0.01% at high generation rates, which is comparable to the reported internal QE of the as-exfoliated WSe_2 monolayer.[24] By applying a small strain of ϵ = 0.5%, the saturated EL QE reached ~8% at maximum (Figure 3B), which exceeds the previously reported transient mode EL device based on chemically counterdoped monolayer TMDC (~1%).[24] Unlike the no-strain device, the EL QE was maintained even at the high carrier injection rates. This efficiency roll-off free performance is attributed to the suppression of EEA by the strain. The reason why EL efficiency is not as high as PL QY is possibly related to the transient electroluminescence mechanism (Figure 3C). When the device reaches steady state, the semiconductor is charged with one polarity of carriers. During the voltage transition, the opposite polarity of the carrier is injected. The two types of carriers create both neutral excitons and charged trions. The exciton and trion concentrations are space and time dependent. As trions recombine nonradiatively, not all carrier recombination results in light emission. This fundamentally limits the highest achievable EL efficiency in transient injection. Figure 3D shows a benchmark of EL external efficiency for TMDC monolayers. The external efficiency of the transient mode in this work is superior to $p-n$ diodes,[6,7,9,13] Schottky diodes,[23] and semiconductor−insulator−semiconductor (SIS)[22] structures and is comparable to an MIS device[21] based on monolayer WS_2 even at the higher generation rates. Here, note that the EL QE is underestimated because of parasitic capacitances and resistances in the device. Also, a built-in strain during the transfer process possibly causes the nonuniform strain distribution in the monolayer, which results in a slight EL efficiency drop at the high generation rates. To further improve the EL QE, it will be helpful to treat TMDC monolayers by chemical counterdoping such as Nafion and bis(trifluoromethane)-sulfonimide,[1,5] together with strain engineering. Although the present EL device has a limited lateral size of several tens of micrometers due to the limitation of the dry transfer process, it can be enlarged to a centimeter-scale with an improvement in the transfer process. Centimeter-scale transfer will be realized via a wet/dry process, from the growth substrate (e.g., SiO_2/Si) to the strain platform used in this work, using supporting polymer layers.[29−31] Toward a wafer-scale EL device on a solid substrate, strain injection in the TMDC monolayer during CVD growth will be useful, with the use of an appropriate growth substrate due to the difference of the thermal expansion coefficient between the monolayer and substrate.[32] Strain-engineered growth has been established with an exploration of various kinds of growth substrates (e.g., silica, AlN, and Al_2O_3), achieving ~1% built-in strain.[32] This built-in strain will simplify the device fabrication process rather than the transfer method so that it will enable more practical applications.

Conventional transient devices are known to suffer from high operating voltages. We show that the onset voltage for EL can be decreased by reducing the dielectric thickness. The gate capacitance is small for thick gate oxides, and the voltage transient can only induce gradual band bending at the contacts. We fabricated devices in which AC voltage is applied between the WSe_2 monolayer and bottom gate across a thin high-k gate dielectric (20 nm thick ZrO_2), as shown in Figure 4A. The source contact pads were kept on relatively thick SiO_2 to reduce parasitic capacitance and improve device robustness. The EL from such a device turns on at a voltage very comparable to the optical band gap (Figure 4B). The lower turn on voltage is observed at a different range to frequencies (Figure 4C), compared to an EL device with a 50 nm gate

https://doi.org/10.1021/acs.nanolett.2c01311
Nano Lett. 2022, 22, 5316−5321

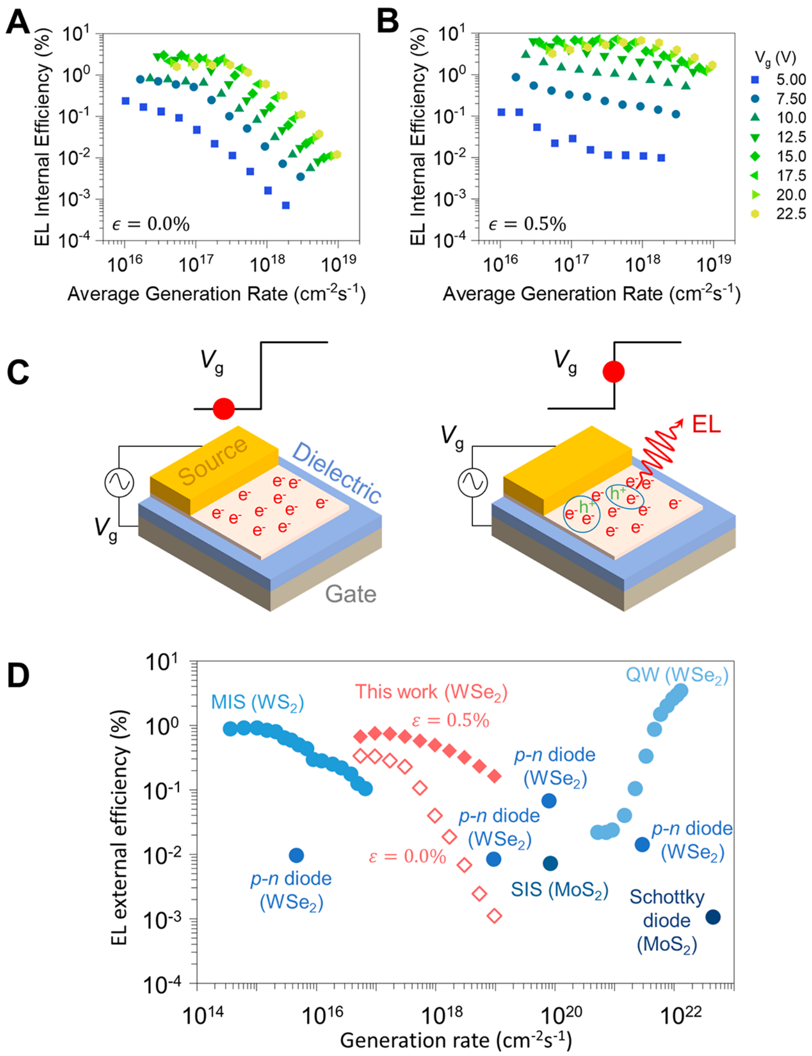

Figure 3. EL internal efficiency in monolayer WSe_2. (A, B) EL internal efficiency in monolayer WSe_2 as a function of injected average carrier density and gate voltage, under different tensile strains of 0.0% and 0.5%, respectively. (C) Fundamental limits of transient EL. (D) Benchmark of EL external efficiency for TMDC monolayers: a comparison with *p*−*n* diode,[6,7,9,13] Schottky diode,[23] SIS,[22] MIS,[21] and QW[15,16] structures.

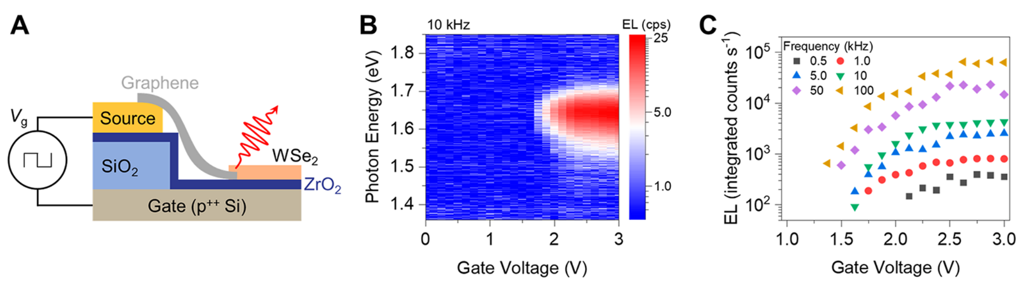

Figure 4. Low-voltage transient EL from WSe_2. (A) Cross-sectional schematic and (B) EL mapping as a function of photon energy and gate voltage. (C) Integrated EL counts showing device turn-on near the gate voltages comparable with the band gap photon energy of monolayer WSe_2.

oxide (Figure S3). We show that EL can be produced with transient voltages comparable to the optical band gap of monolayer semiconductors and on par with the voltages in DC EL devices.[26]

In conclusion, a dynamically strain tunable flexible device was fabricated with the conventional gate oxide and TMDC monolayers of WS_2 and WSe_2. Although the transient-mode EL device of monolayer WSe_2 under no strain revealed an efficiency roll-off at the high injection carrier density, an efficiency roll-off free EL device was achieved by applying a small tensile strain, which suppresses the EEA. The present results will be useful for practical optoelectrical devices such as light sources, photodetectors, and energy harvesting platforms.

METHODS

Device Fabrication. The strain tunable devices for PL and EL measurements were fabricated on a polyimide substrate (Kapton, Dupont, 1.5 mm thickness). Ti (10 nm)/Au (100 nm)/Ti (10 nm) was fabricated as back gate electrodes using standard photolithography and thermal evaporation. As a gate

https://doi.org/10.1021/acs.nanolett.2c01311
Nano Lett. 2022, 22, 5316−5321

insulator, 50 nm Al_2O_3 was deposited via ALD at 200 °C. For an EL device with a thin high-*k* gate dielectric, 20 nm ZrO_2 was deposited via ALD at 180 °C after opening SiO_2 windows in 50 nm SiO_2/p^{++}-Si substrate. 50 nm thick Au source electrodes were patterned on ALD oxide. WS_2 and WSe_2 monolayers were grown on SiO_2/Si substrate via CVD. The detailed growth processes for WS_2 and WSe_2 are described in previously reported papers.[25,32] Monolayer films were picked up with poly(methyl methacrylate) (PMMA) and transferred onto the ALD oxide, followed by a post-baking at 180 °C for 5 min and dichloromethane treatment to remove PMMA. As a source contact, mechanically exfoliated multilayer graphene (Graphenium, NGS Naturgraphit) was dry-transferred with PMMA to mediate between the Au electrode pad and monolayer. Another post-baking (180 °C, 5 min) was performed to improve the adhesion between the interfaces of TMDC/oxide and graphene/TMDC.

Electrical and Optical Characterization. Devices were charged from a Keithley 2410 source meter applied to the gate electrode while the Au source was grounded. The calibrated PL QY was measured using a home-built micro-PL instrument described in detail in the previous study.[1,2,5] A 514.5 nm line was used as the excitation source. A uniaxial tensile strain was applied in the monolayer by a two-point linear actuator. The nominal applied strain was calculated using the equation $\varepsilon = t/R$, where $2t$ and R are the substrate thickness and curvature radius measured through the cross-section optical image. For PL QY calibration, the wavelength of the spectrometer was verified with Arlamps (Newport), and the wavelength-dependent instrument response function was measured by a virtual Lambertian blackbody source, which was created with a stabilized lamp (Thorlabs SLS201) and a Spectralon reflection standard (Labsphere). The collection efficiency was then acquired by measuring the laser response which was focused on the Spectralon reflection standard. The pump−power dependence is converted to QY by dividing the CCD counts (N) by the product of pump power (P) and coupling factor (F), i.e.: $QY = N/(FP)$. Because the emission profile of the monolayer semiconductors has been known to be Lambertian, this gives the reasonable approximation of the source of PL emission from the monolayers. EL spectra were measured using a bipolar wave from an Agilent 33522A arbitrary waveform generator applied to the gate electrode, while the source contact was grounded. All measurements reported in this paper are taken at room temperature in an ambient lab condition under nitrogen flow.

ASSOCIATED CONTENT

Supporting Information

The Supporting Information is available free of charge at https://pubs.acs.org/doi/10.1021/acs.nanolett.2c01311.

Electrical and optical characterization methods; typical PL spectra of monolayer WS_2 under different uniaxial strains; PL QY in monolayer WS_2 at different generation rates, gate voltages, and strain; and gate voltage dependence of integrated EL counts under no strain for the transient mode WSe_2 EL device (PDF)

AUTHOR INFORMATION

Corresponding Author

Ali Javey − *Electrical Engineering and Computer Sciences, University of California, Berkeley, California 94720, United States; Materials Sciences Division, Lawrence Berkeley National Laboratory, Berkeley, California 94720, United States;* orcid.org/0000-0001-7214-7931; Email: ajavey@berkeley.edu

Authors

Shiekh Zia Uddin − *Electrical Engineering and Computer Sciences, University of California, Berkeley, California 94720, United States; Materials Sciences Division, Lawrence Berkeley National Laboratory, Berkeley, California 94720, United States;* orcid.org/0000-0002-1265-9940

Naoki Higashitarumizu − *Electrical Engineering and Computer Sciences, University of California, Berkeley, California 94720, United States; Materials Sciences Division, Lawrence Berkeley National Laboratory, Berkeley, California 94720, United States;* orcid.org/0000-0003-3996-6753

Hyungjin Kim − *Electrical Engineering and Computer Sciences, University of California, Berkeley, California 94720, United States; Materials Sciences Division, Lawrence Berkeley National Laboratory, Berkeley, California 94720, United States*

I. K. M. Reaz Rahman − *Electrical Engineering and Computer Sciences, University of California, Berkeley, California 94720, United States; Materials Sciences Division, Lawrence Berkeley National Laboratory, Berkeley, California 94720, United States*

Complete contact information is available at: https://pubs.acs.org/10.1021/acs.nanolett.2c01311

Author Contributions

[†]S.Z.U. and N.H. contributed equally. S.Z.U., H.K., N.H., and A.J. conceived the idea for the project and designed the experiments. N.H. and I.K.M.R.R. performed CVD growth of TMDC monolayers. S.Z.U. and N.H. fabricated devices, performed optical measurements. S.Z.U., N.H., and A.J. analyzed the data. S.Z.U., N.H., and A.J. wrote the manuscript. All authors discussed the results and commented on the manuscript.

Notes

The authors declare no competing financial interest.

ACKNOWLEDGMENTS

This work is supported by the Director, Office of Science, Office of Basic Energy Sciences, Materials Sciences and Engineering Division of the U.S. Department of Energy, under contract DE-AC02-05Ch11231. H.K. acknowledges support from Samsung Scholarship. N.H. acknowledges support from the Postdoctoral Fellowships for Research Abroad of Japan Society for the Promotion of Science.

REFERENCES

(1) Amani, M.; Lien, D.-H.; Kiriya, D.; Xiao, J.; Azcatl, A.; Noh, J.; Madhvapathy, S. R.; Addou, R.; Kc, S.; Dubey, M.; Cho, K.; Wallace, R. M.; Lee, S.-C.; He, J.-H.; Ager, J. W., 3rd; Zhang, X.; Yablonovitch, E.; Javey, A. Near-Unity Photoluminescence Quantum Yield in MoS_2. *Science* **2015**, *350* (6264), 1065−1068.

(2) Lien, D.-H.; Uddin, S. Z.; Yeh, M.; Amani, M.; Kim, H.; Ager, J. W., 3rd; Yablonovitch, E.; Javey, A. Electrical Suppression of All Nonradiative Recombination Pathways in Monolayer Semiconductors. *Science* **2019**, *364* (6439), 468−471.

(3) Murawski, C.; Leo, K.; Gather, M. C. Efficiency Roll-off in Organic Light-Emitting Diodes. *Adv. Mater.* **2013**, *25* (47), 6801−6827.

(4) Bae, W. K.; Park, Y.-S.; Lim, J.; Lee, D.; Padilha, L. A.; McDaniel, H.; Robel, I.; Lee, C.; Pietryga, J. M.; Klimov, V. I. Controlling the Influence of Auger Recombination on the Performance of Quantum-Dot Light-Emitting Diodes. *Nat. Commun.* **2013**, *4* (1), 2661.

(5) Kim, H.; Uddin, S. Z.; Higashitarumizu, N.; Rabani, E.; Javey, A. Inhibited Nonradiative Decay at All Exciton Densities in Monolayer Semiconductors. *Science* **2021**, *373* (6553), 448−452.

(6) Zhang, Y. J.; Oka, T.; Suzuki, R.; Ye, J. T.; Iwasa, Y. Electrically Switchable Chiral Light-Emitting Transistor. *Science* **2014**, *344* (6185), 725−728.

(7) Baugher, B. W. H.; Churchill, H. O. H.; Yang, Y.; Jarillo-Herrero, P. Optoelectronic Devices Based on Electrically Tunable *p-n* Diodes in a Monolayer Dichalcogenide. *Nat. Nanotechnol.* **2014**, *9* (4), 262−267.

(8) Jo, S.; Ubrig, N.; Berger, H.; Kuzmenko, A. B.; Morpurgo, A. F. Mono- and Bilayer WS_2 Light-Emitting Transistors. *Nano Lett.* **2014**, *14* (4), 2019−2025.

(9) Ross, J. S.; Klement, P.; Jones, A. M.; Ghimire, N. J.; Yan, J.; Mandrus, D. G.; Taniguchi, T.; Watanabe, K.; Kitamura, K.; Yao, W.; Cobden, D. H.; Xu, X. Electrically Tunable Excitonic Light-Emitting Diodes Based on Monolayer WSe_2 *p-n* Junctions. *Nat. Nanotechnol.* **2014**, *9* (4), 268−272.

(10) Lopez-Sanchez, O.; Alarcon Llado, E.; Koman, V.; Fontcuberta i Morral, A.; Radenovic, A.; Kis, A. Light Generation and Harvesting in a van Der Waals Heterostructure. *ACS Nano* **2014**, *8* (3), 3042−3048.

(11) Ye, Y.; Ye, Z.; Gharghi, M.; Zhu, H.; Zhao, M.; Wang, Y.; Yin, X.; Zhang, X. Exciton-Dominant Electroluminescence from a Diode of Monolayer MoS_2. *Appl. Phys. Lett.* **2014**, *104* (19), 193508.

(12) Cheng, R.; Li, D.; Zhou, H.; Wang, C.; Yin, A.; Jiang, S.; Liu, Y.; Chen, Y.; Huang, Y.; Duan, X. Electroluminescence and Photocurrent Generation from Atomically Sharp WSe_2/MoS_2 Heterojunction *p-n* Diodes. *Nano Lett.* **2014**, *14* (10), 5590−5597.

(13) Pospischil, A.; Furchi, M. M.; Mueller, T. Solar-Energy Conversion and Light Emission in an Atomic Monolayer *p-n* Diode. *Nat. Nanotechnol.* **2014**, *9* (4), 257−261.

(14) Yang, W.; Shang, J.; Wang, J.; Shen, X.; Cao, B.; Peimyoo, N.; Zou, C.; Chen, Y.; Wang, Y.; Cong, C.; Huang, W.; Yu, T. Electrically Tunable Valley-Light Emitting Diode (VLED) Based on CVD-Grown Monolayer WS_2. *Nano Lett.* **2016**, *16* (3), 1560−1567.

(15) Withers, F.; Del Pozo-Zamudio, O.; Schwarz, S.; Dufferwiel, S.; Walker, P. M.; Godde, T.; Rooney, A. P.; Gholinia, A.; Woods, C. R.; Blake, P.; Haigh, S. J.; Watanabe, K.; Taniguchi, T.; Aleiner, I. L.; Geim, A. K.; Fal'ko, V. I.; Tartakovskii, A. I.; Novoselov, K. S. Wse_2 Light-Emitting Tunneling Transistors with Enhanced Brightness at Room Temperature. *Nano Lett.* **2015**, *15* (12), 8223−8228.

(16) Withers, F.; Del Pozo-Zamudio, O.; Mishchenko, A.; Rooney, A. P.; Gholinia, A.; Watanabe, K.; Taniguchi, T.; Haigh, S. J.; Geim, A. K.; Tartakovskii, A. I.; Novoselov, K. S. Light-Emitting Diodes by Band-Structure Engineering in van Der Waals Heterostructures. *Nat. Mater.* **2015**, *14* (3), 301−306.

(17) Liu, C.-H.; Clark, G.; Fryett, T.; Wu, S.; Zheng, J.; Hatami, F.; Xu, X.; Majumdar, A. Nanocavity Integrated van Der Waals Heterostructure Light-Emitting Tunneling Diode. *Nano Lett.* **2017**, *17* (1), 200−205.

(18) Kim, Y. D.; Kim, H.; Cho, Y.; Ryoo, J. H.; Park, C.-H.; Kim, P.; Kim, Y. S.; Lee, S.; Li, Y.; Park, S.-N.; Yoo, Y. S.; Yoon, D.; Dorgan, V. E.; Pop, E.; Heinz, T. F.; Hone, J.; Chun, S.-H.; Cheong, H.; Lee, S. W.; Bae, M.-H.; Park, Y. D. Bright Visible Light Emission from Graphene. *Nat. Nanotechnol.* **2015**, *10* (8), 676−681.

(19) Kim, Y. D.; Gao, Y.; Shiue, R.-J.; Wang, L.; Aslan, O. B.; Bae, M.-H.; Kim, H.; Seo, D.; Choi, H.-J.; Kim, S. H.; Nemilentsau, A.; Low, T.; Tan, C.; Efetov, D. K.; Taniguchi, T.; Watanabe, K.; Shepard, K. L.; Heinz, T. F.; Englund, D.; Hone, J. Ultrafast Graphene Light Emitters. *Nano Lett.* **2018**, *18* (2), 934−940.

(20) Palacios-Berraquero, C.; Barbone, M.; Kara, D. M.; Chen, X.; Goykhman, I.; Yoon, D.; Ott, A. K.; Beitner, J.; Watanabe, K.; Taniguchi, T.; Ferrari, A. C.; Atatüre, M. Atomically Thin Quantum Light-Emitting Diodes. *Nat. Commun.* **2016**, *7* (1), 12978.

(21) Wang, S.; Wang, J.; Zhao, W.; Giustiniano, F.; Chu, L.; Verzhbitskiy, I.; Zhou Yong, J.; Eda, G. Efficient Carrier-to-Exciton Conversion in Field Emission Tunnel Diodes Based on MIS-Type van Der Waals Heterostack. *Nano Lett.* **2017**, *17* (8), 5156−5162.

(22) Li, D.; Cheng, R.; Zhou, H.; Wang, C.; Yin, A.; Chen, Y.; Weiss, N. O.; Huang, Y.; Duan, X. Electric-Field-Induced Strong Enhancement of Electroluminescence in Multilayer Molybdenum Disulfide. *Nat. Commun.* **2015**, *6*, 7509.

(23) Sundaram, R. S.; Engel, M.; Lombardo, A.; Krupke, R.; Ferrari, A. C.; Avouris, P.; Steiner, M. Electroluminescence in Single Layer MoS_2. *Nano Lett.* **2013**, *13* (4), 1416−1421.

(24) Lien, D.-H.; Amani, M.; Desai, S. B.; Ahn, G. H.; Han, K.; He, J.-H.; Ager, J. W., 3rd; Wu, M. C.; Javey, A. Large-Area and Bright Pulsed Electroluminescence in Monolayer Semiconductors. *Nat. Commun.* **2018**, *9* (1), 1229.

(25) Cho, J.; Amani, M.; Lien, D.; Kim, H.; Yeh, M.; Wang, V.; Tan, C.; Javey, A. Centimeter-scale and Visible Wavelength Monolayer Light-emitting Devices. *Adv. Funct. Mater.* **2020**, *30* (6), 1907941.

(26) Wang, V.; Zhao, Y.; Javey, A. Performance Limits of an Alternating Current Electroluminescent Device. *Adv. Mater.* **2021**, *33* (2), e2005635.

(27) Zhao, Y.; Wang, V.; Lien, D.-H.; Javey, A. A Generic Electroluminescent Device for Emission from Infrared to Ultraviolet Wavelengths. *Nat. Electron.* **2020**, *3* (10), 612−621.

(28) Uddin, S. Z.; Higashitarumizu, N.; Kim, H.; Rabani, E.; Javey, A. Engineering Exciton Recombination Pathways in Bilayer WSe_2 for Bright Luminescence. *ACS Nano* **2022**, *16* (1), 1339.

(29) Tsai, M.-L.; Su, S.-H.; Chang, J.-K.; Tsai, D.-S.; Chen, C.-H.; Wu, C.-I.; Li, L.-J.; Chen, L.-J.; He, J.-H. Monolayer MoS_2 Heterojunction Solar Cells. *ACS Nano* **2014**, *8* (8), 8317−8322.

(30) Watson, A. J.; Lu, W.; Guimarães, M. H. D.; Stöhr, M. Transfer of Large-Scale Two-Dimensional Semiconductors: Challenges and Developments. *2d Mater.* **2021**, *8* (3), 032001.

(31) Nguyen, V.; Gramling, H.; Towle, C.; Li, W.; Lien, D.-H.; Kim, H.; Chrzan, D. C.; Javey, A.; Xu, K.; Ager, J.; Taylor, H. Deterministic Assembly of Arrays of Lithographically Defined WS_2 and MoS_2 Monolayer Features Directly From Multilayer Sources Into Van Der Waals Heterostructures. *J. Micro Nano-Manuf* **2019**, *7* (4), 041006.

(32) Ahn, G. H.; Amani, M.; Rasool, H.; Lien, D.-H.; Mastandrea, J. P.; Ager, J. W., III; Dubey, M.; Chrzan, D. C.; Minor, A. M.; Javey, A. Strain-Engineered Growth of Two-Dimensional Materials. *Nat. Commun.* **2017**, *8* (1), 608.

https://doi.org/10.1021/acs.nanolett.2c01311
Nano Lett. 2022, 22, 5316−5321